Thermal Resistance Network Derivative (TREND) Model for Efficient Thermal Simulation and Design of ICs and Packages

Shunxiang Lan
State Key Laboratory of Radio Frequency Heterogeneous Integration, SJTU
Shanghai, China
showbeone@sjtu.edu.cn

Min Tang
State Key Laboratory of Radio Frequency Heterogeneous Integration, SJTU
Shanghai, China
tm222@sjtu.edu.cn

Liang Chen
School of Microelectronics, Shanghai University
Shanghai, China
lchenshu@shu.edu.cn

Junfa Mao
State Key Laboratory of Radio Frequency Heterogeneous Integration, SJTU
Shanghai, China
jfmao@sjtu.edu.cn

ABSTRACT

In the thermal design of 3-D integrated circuits (ICs) and packages, numerical simulation is extensively employed to investigate the impact of model parameters on hotspot temperature. However, conventional simulation approaches usually require plenty of computational resource and thus lead to expensive time cost for thermal designs. In this paper, we present a novel technique to efficiently and accurately conduct thermal simulation of 3-D ICs and packages, potentially reducing thermal design timeline from weeks to minutes. The proposed thermal resistance network derivative (TREND) model facilitates to focus the solution domain on the crucial regions for thermal designs and accelerate simulation without sacrificing accuracy. Also, the TREND model protects the internal details of chips and packages, which is quite suitable for modular thermal designs. The flexibility, accuracy, and efficiency of the proposed method are demonstrated through several numerical examples. Compared with the commercial software, a speed-up of 2695x is achieved in a typical thermal design case without the loss of accuracy.

1 INTRODUCTION

The advent of 3-D integrated circuits (ICs) and packages presents an exceedingly compelling solution to overcome the interconnect bottleneck in the design of highly integrated systems [1]. However, the power density in multi-layer stacked structures is dramatically increased, which leads to an increase of hotspot temperature, also resulting in circuit functionality degradation and thermal stress concerns [2]. Therefore, thermal analysis and management have gradually emerged as essential components in the design of 3-D ICs and packages for maximizing the performance, reliability, and lifetime [3].

DAC '24, June 23–27, 2024, San Francisco, CA, USA

ACM ISBN 979-8-4007-0601-1/24/06
https://doi.org/10.1145/3649329.3657366

In the thermal design of 3-D ICs and packages, the hotspot temperature serves as a crucial indicator for evaluating the adequacy. A commonly used method for the optimal thermal design involves performing extensive thermal simulations to investigate the impact of model parameters on the hotspot temperature [4–6]. Nevertheless, vast temperature data from simulations is usually unnecessary for thermal design, as the hotspot temperature usually occurs within a small region which contains information of heat source. This undoubtedly leads to a substantial waste of computational resources and imposes high time costs.

One possible approach to tackle this problem is to convert the inherent heat transfer characteristics of the fixed regions into equivalent thermal boundary conditions on the surfaces of the regions which are crucial for thermal design. By this means, thermal simulations can be performed exclusively within the domains of interest for the thermal design, thus reducing the computational resources significantly.

In [7], a novel concept of adiabatic heat transfer coefficient is proposed and compared to the typical heat transfer coefficient. Subsequently, research is conducted on the calculation of the adiabatic heat transfer coefficient [8], [9], which can also be applied to decouple convection and conductive heat transfer [10]. Moreover, it is further applied to describe the interplay of conjugate heat transfer between protruding heaters in air-forced convection cooling [11–13]. However, this kind of methods are solely applicable to temperature prediction for isothermal heater blocks and fail to meet the requirement of complicated thermal simulation for ICs and packages.

In recent years, the boundary condition independent (BCI) compact thermal model (CTM) has been presented for efficient thermal simulation [14]. By extracting the parameters from an appropriate set of boundary conditions and combining with a multi-point moment matching approach [15–17], BCI CTM can approximate the thermal behavior of electronic packages with desired level of accuracy [18–20]. Nevertheless, this approach inevitably entails certain degrees of accuracy loss.

To overcome the aforementioned limitation, we propose a novel technique for efficient thermal simulation and design of ICs and packages based on the thermal resistance derivative (TREND) model. The main contributions of this work are described as follows:

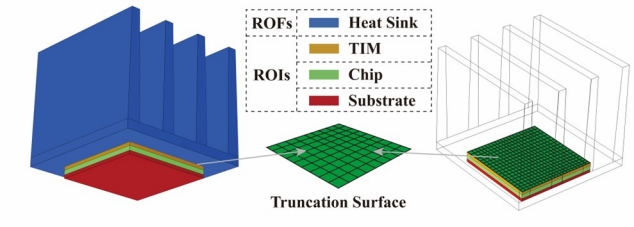

Figure 1: Schematic of region decomposition strategy for ICs and packages.

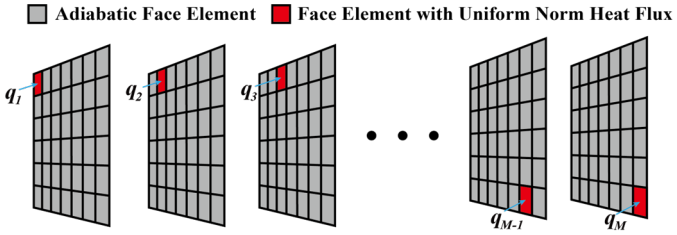

Figure 2: The process of applying heat flux density excitation on the truncation surface.

- We introduce an instructive strategy of region decomposition for thermal design of 3-D ICs and packages. It partitions the entire model into several distinct subregions based on the specific structural characteristics and the key indicators for thermal design. It establishes the foundation for the efficient simulation of crucial regions and enables the potential for parallel computation.
- We propose a novel TREND model to effectively and precisely describe the inherent heat transfer characteristic of the fixed regions. The model can be utilized to construct equivalent thermal boundary conditions on the surface of the crucial regions for thermal design, reducing the solution domain and thereby speeding up the simulation without sacrificing accuracy. In addition, the TREND model can protect the internal details of chips and packages, and its merit of reusability facilitates the modular thermal design.
- We demonstrate the characteristics and advantages of the proposed method by two typical examples. Firstly, we illustrate how to take advantage of the invariance of heat transfer system to reuse the TREND model and facilitate flexible modular thermal design. Secondly, the accuracy and efficiency of the proposed method are validated by the thermal design of a complicated structure of 3-D ICs and packages with microchannel heat sink. Compared with the commercial software, the proposed method can achieve a significant speed-up without the loss of accuracy.

2 PROPOSED METHOD

2.1 Region Decomposition Strategy

According to the specific requirements of thermal design for 3-D ICs and packages, the whole structure can be divided into two parts: regions of interest (ROIs) and regions of fixity (ROFs), which is demonstrated in Figure 1. The ROIs usually contain prominent components with high power density, and the hotspot temperature within ROIs generally serves as the most interesting indicator for thermal design. On the other hand, the ROFs typically consist of the cooling system which remains fixed throughout the entire process of thermal design. To be more specific, the instructive strategy for setting the ROIs and ROFs is summarized as follows.

(1) The ROIs contain all crucial temperature distributions for thermal design.
(2) The heat transfer characteristics of ROFs keep unchanged during the thermal design, satisfying the requirement of a linear time-invariant system.
(3) The variation of parameters related to thermal design only occurs within the ROIs and it do not affect the relative position of the truncation surfaces of the ROFs.

2.2 TREND Model

To construct equivalent thermal boundary conditions on the truncation surfaces of the ROIs and ROFs, we present a novel TREND model. For simplicity without loss of generality, the steady-state heat transfer problem of a ROF is considered to demonstrate the main process.

Firstly, the ROF is spatially discretized using finite volume method (FVM), resulting in orthogonal gird on the truncation surface shown in Figure 1.

Then, by imposing the adiabatic boundary condition to the truncation surface, we set up a matrix equation for the ROF as

$$\boldsymbol{A}\boldsymbol{x} = \boldsymbol{b} \tag{1}$$

where $\boldsymbol{A}$ is the stiffness matrix, $\boldsymbol{b}$ is the right-hand side vector, and $\boldsymbol{x}$ is the solution vector. Assuming that there are M face elements on the truncation surface, we solve the above matrix equation to obtain the temperature $\boldsymbol{T}^{ad}$ on the truncation surface, which is an $M \times 1$ vector.

Next, a uniform heat flux density excitation is imposed on the face elements one by one. The process is illustrated in Figure 2. The magnitude of the heat flux density applied on the j-th ($j = 1, 2, \cdots, M$) face element is denoted as q_j, and the resulting temperature distribution on the truncation surface is denoted as $\boldsymbol{T}_j$. It is worth noting that the heat flux density excitation on the truncation surface only affects the value of $\boldsymbol{b}$ in (1), while the matrix $\boldsymbol{A}$ remains unchanged. Therefore, when a sparse linear direct solver is employed (e.g., PARDISO-LU [21]), it is convenient to reuse the LU decomposition information of $\boldsymbol{A}$ to accelerate the thermal simulation.

After $\boldsymbol{T}^{ad}$, q_j and $\boldsymbol{T}_j$ are obtained, we define the equivalent transfer thermal resistance R_{ij} from the j-th face element to the i-th ($i = 1, 2, \cdots, M$) face element on the truncation surface as:

$$R_{ij} = \frac{\boldsymbol{T}_j(i) - \boldsymbol{T}^{ad}(i)}{q_j} \tag{2}$$

where $\boldsymbol{T}_j(i)$ denotes the temperature of the center node at the i-th face element when the j-th face element is excited by q_j, and $\boldsymbol{T}^{ad}(i)$ is the adiabatic temperature of the center node at the i-th face element. Based on the principle of superposition, the relationship between the temperature distribution and the normal heat flux distribution on the truncation surface can be further written in a

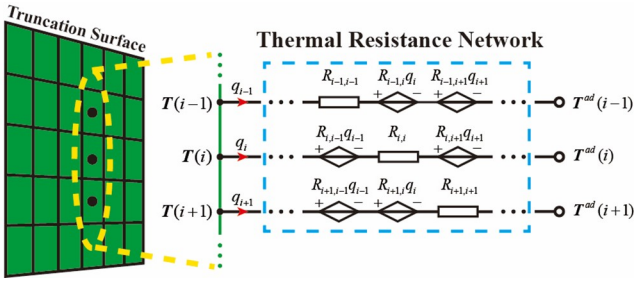

Figure 3: Schematic of the thermal resistance network derivative model.

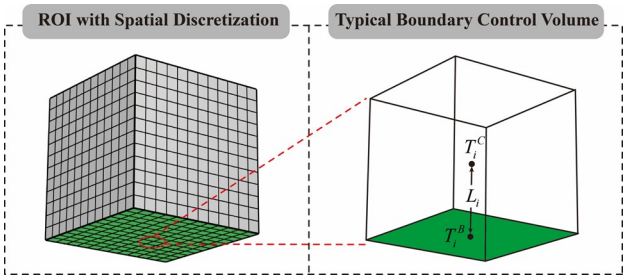

Figure 4: Schematic of a control volume adjacent to the truncation surface.

matrix form as

$$\boldsymbol{T} - \boldsymbol{T}^{ad} = \boldsymbol{R} \cdot \boldsymbol{q} \tag{3}$$

where $\boldsymbol{T}$ is an $M \times 1$ vector denoting the temperature value when all face elements on the truncation surface are simultaneously excited, $\boldsymbol{R}$ is an $M \times M$ matrix and $\boldsymbol{q}$ is an $M \times 1$ vector denoting the magnitude of the normal heat flux density on the truncation surface. Based on (3), we build the TREND model as described in Figure 3. The temperature rise comes from two aspects: self-heating and mutual heating. The self-heating part is the temperature rise $R_{ii} \times q_i$ induced by the local face element's excitation q_i. The mutual heating one is the sum of temperature rise $R_{ij} \times q_j$ induced by other face element's excitation q_j $(j \neq i)$. According to the analogy between the thermal field and electric field, the current-controlled voltage source can be utilized to represent the mutual heating effect, as shown in Figure 3.

Note that since the TREND model is uniquely determined by the material properties, boundary conditions, and geometric shape within ROFs, it can characterize the inherent heat transfer properties of the ROFs and is not dependent on the excitation value of $\boldsymbol{q}$. In addition, if an object consists of several separated ROFs, the establishment of their TREND models can be implemented in parallel to improve the efficiency.

2.3 Equivalent Boundary Conditions

After the TREND model is set up for the ROF, we then need to address the newly boundary-value problem of ROI with the equivalent thermal boundary conditions described as (3). For illustration, a typical example with the orthogonal boundary grid is investigated.

The position of temperature node is set at the center of the control volume for spatial discretization in the FVM. As shown in Figure 4, T_i^C represents the temperature variable of the control volume adjacent to the i-th face element on the truncation surface. To calculate the heat flux density of the boundary face element, an auxiliary variable T_i^B on the truncation surface is introduced. Then, the normal heat flux density q_i on the i-th face element can be calculated by:

$$q_i = -\frac{\kappa_i}{L_i}(T_i^B - T_i^C) \tag{4}$$

where κ_i is the thermal conductivity of the i-th face element on the truncation surface and L_i is the distance from the center of the i-th face element to the center of the adjacent control volume.

Combining (3) and (4), we obtain the following equation,

$$\boldsymbol{T}^B = (\boldsymbol{I} + \boldsymbol{R} \cdot \boldsymbol{D})^{-1} \boldsymbol{R} \cdot \boldsymbol{D} \cdot \boldsymbol{T}^C + (\boldsymbol{I} + \boldsymbol{R} \cdot \boldsymbol{D})^{-1} \boldsymbol{T}^{ad} \tag{5}$$

where $\boldsymbol{I}$ is an $M \times M$ identity matrix and $\boldsymbol{D}$ is an $M \times M$ diagonal matrix described as

$$\boldsymbol{D} = \begin{bmatrix} \kappa_1/L_1 & 0 & \cdots & 0 \\ 0 & \kappa_2/L_2 & \cdots & 0 \\ \vdots & \vdots & \ddots & \vdots \\ 0 & 0 & \cdots & \kappa_M/L_M \end{bmatrix}. \tag{6}$$

From (4)-(6), we can construct the relationship between $\boldsymbol{T}^C$ and $\boldsymbol{q}$ as follows,

$$\boldsymbol{q} = \boldsymbol{f}_1 \cdot \boldsymbol{T}^C + \boldsymbol{f}_2 \tag{7}$$

where

$$\boldsymbol{f}_1 = \boldsymbol{D}[\boldsymbol{I} - (\boldsymbol{I} + \boldsymbol{R} \cdot \boldsymbol{D})^{-1} \boldsymbol{R} \cdot \boldsymbol{D}]$$
$$\boldsymbol{f}_2 = -\boldsymbol{D}(\boldsymbol{I} + \boldsymbol{R} \cdot \boldsymbol{D})^{-1} \boldsymbol{T}^{ad}$$

Subsequently, the relation (7) will be treated as the Robin boundary conditions in the following thermal simulation. Assuming that there are N_F control volumes within ROF and N_I control volumes within ROI, the degree of freedom (DoF) of the linear system for the entire solution domain is $N_F + N_I$, while the DoF of linear system for ROI is only N_I. Thus, the proposed method can accelerate the thermal simulation by reducing the solution domain without sacrificing accuracy.

3 NUMERICAL RESULTS

Several numerical examples are presented to validate the accuracy and efficiency of the proposed method, as well as the flexible modular thermal design. All the numerical examples are performed on a server with two Intel Xeon Platinum 8268 CPUs (2.90 GHz/2.89 GHz) and 1.0-TB memory.

3.1 Modular Thermal Design of 2-D Structures

In the first example, a simple 2-D case consisting of four regions (A, B, C and D) is investigated, as shown in Figure 5. These regions contain different materials, and their respective thermal conductivity is listed in Table 1. Since the material in region C is fluid with velocity, the whole system is associated with the conjugate heat transfer analysis.

The boundary conditions and heat source of the structure are given as follows. In region A, the left edge is set as a constant temperature boundary with $T_A = 30$ ℃. In region B, the upper edge is set as a convection boundary with a convection coefficient $h_f = 0.001$ W/(mm· K) and an ambient temperature of $T_B = 25$ ℃. In region C, the lower edge is set as a constant temperature boundary with $T_C = 20$ ℃ and the flow velocity u is assumed to be

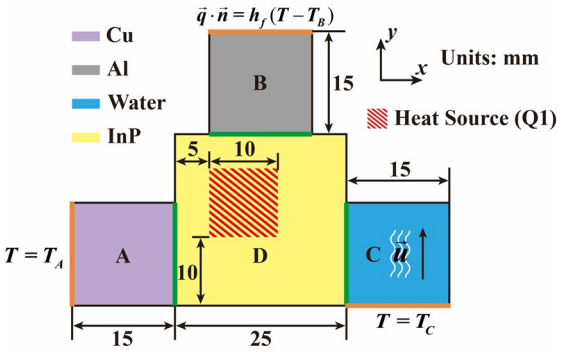

Figure 5: A 2-D case consisting of four regions (A, B, C, and D).

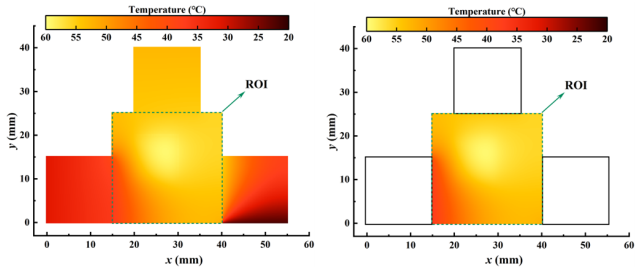

Figure 6: Temperature distributions of the first case in (a) the whole structure obtained by FLUENT and (b) the ROI obtained by the proposed method.

Table 1: Thermal conductivity of materials

Material	Thermal Conductivity $(W/(m \cdot K))$
Copper	400
Aluminum	202.4
InP	68
Silicon	130
Water	0.575

parallel to the truncation surface with a magnitude of 0.001 mm/s. All other boundaries are set to be adiabatic. In region D, the heat source density is Q1 = 0.03 W/mm^2, which is uniformly distributed.

Assuming that we are only interested in the temperature distribution in the region D for thermal design, we can consider region D as the ROI while treating regions A, B, and C as the ROFs.

For comparison, the steady-state thermal simulation is performed by ANSYS FLUENT [22] and the proposed method, respectively. The temperature distribution of the whole structure by FLUENT is shown in Figure 6(a). With the proposed method, the result in the ROI is illustrated in Figure 6(b). It is evident that the thermal profiles of the ROI are in good agreement with each other. The maximum absolute error is less than 10^{-5} ℃.

Then, in order to verify the reusability of the TREND model, we investigate another 2-D structure, as shown in Figure 7. It also holds four regions, where regions A, B, and C are the same to the previous ones. In region E, the density of heat source is Q2 = 0.05 W/mm^2, and the upper boundary is imposed with a heat flux density q_E = 0.001 W/mm. Note that since the regions A, B,

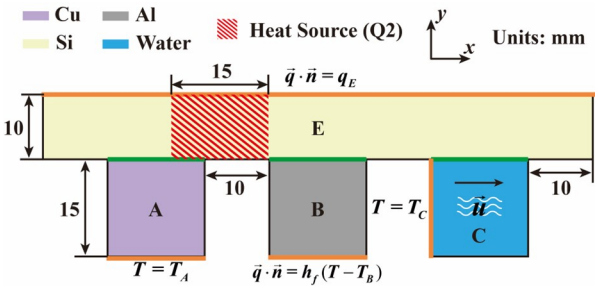

Figure 7: Another 2-D case consisting of four regions (A, B, C, and E).

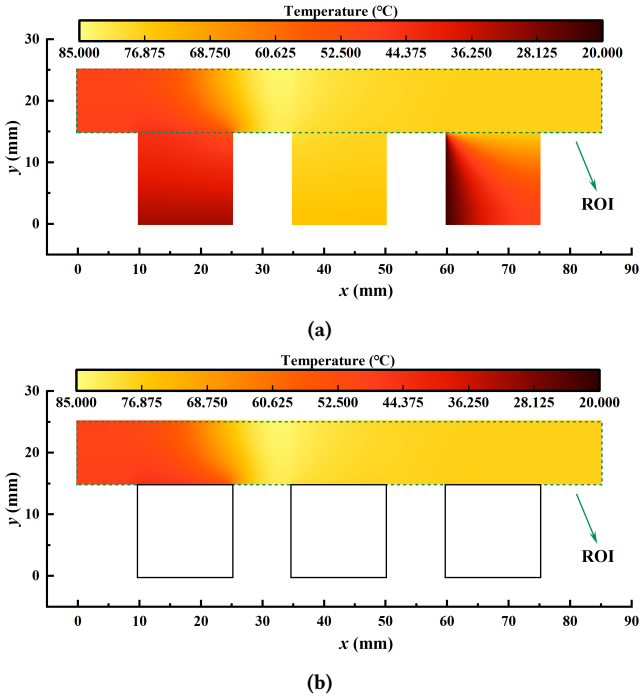

Figure 8: Temperature distributions of the second case in (a) the entire domain obtained by FLUENT and (b) the ROI obtained by the proposed method.

and C remain unchanged, there is no need to reestablish their TREND models. Thus, the internal details of these regions can be successfully protected in the process of thermal design. The simulated results are compared in Figure 8. It is shown that the temperature distributions match remarkably well and the maximum absolute error is less than 10^{-5} ℃.

Based on the above analysis, it is evident that we can arbitrarily change the intensity and position of the heat source, material properties, boundary conditions and geometric topology within the ROI as long as these changes do not affect the relative position of the truncation surfaces of the ROFs. Moreover, the reusability of the TREND model allows for flexible modular design with arbitrary combination and arrangement.

3.2 3-D ICs with Microchannel Heat Sink

To evaluate the accuracy and efficiency of the proposed method for thermal design, a complicated system consisting of 3-D ICs [4]

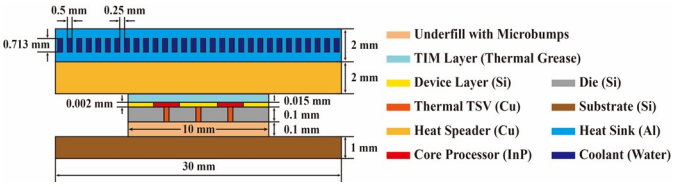

Figure 9: Schematic of the cross-section of the nominal 3-D ICs with MCHS.

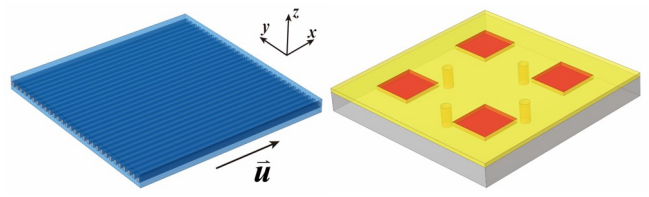

(a) (b)

Figure 10: 3-D display of (a) the MCHS and (b) the nominal arrangement of TSVs.

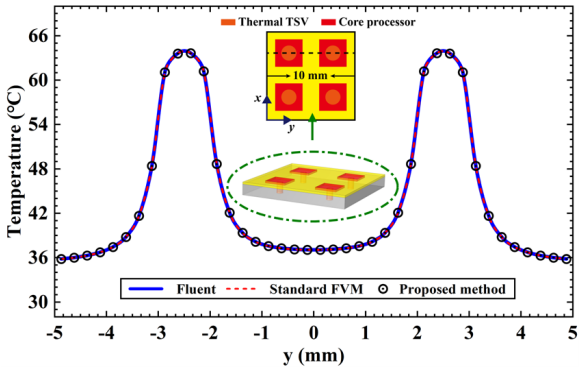

(a)

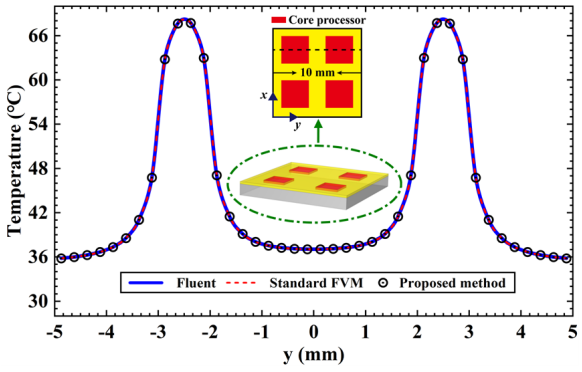

(b)

Figure 11: The temperature profile in the device layer with different arrangements, (a) core-concentrated TSV case, and (b) no TSV case.

with a microchannel heat sink (MCHS) [23] is considered in this example, as shown in Figure 9. The 3-D display of the MCHS and the nominal arrangement of TSVs is provided in Figure 10.

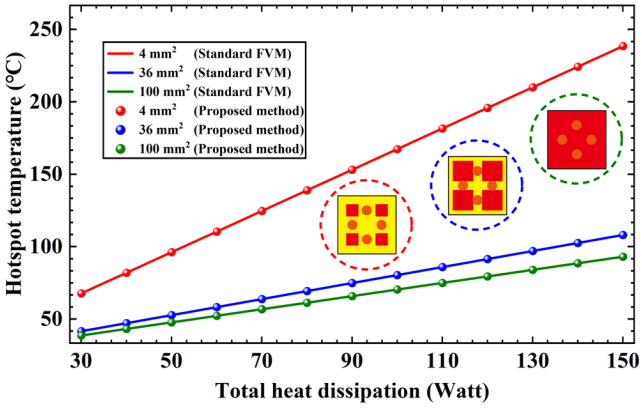

(a)

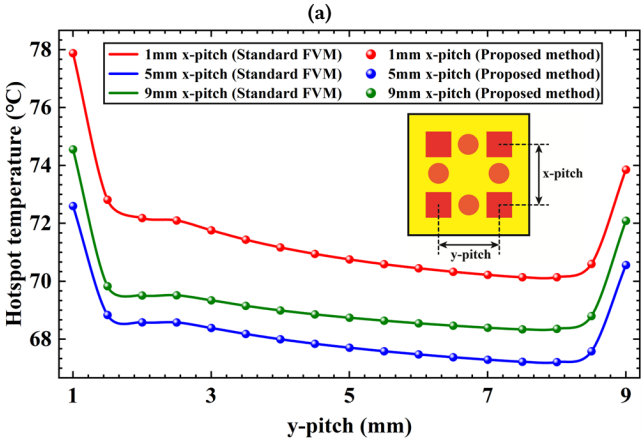

(b)

Figure 12: (a) Effect of processor area and heat dissipation. (b) Effect of processor pitch with the heat dissipation of 30 W.

In the thermal analysis of conjugate heat transfer involved in this example, the boundary conditions of the flow field in microchannel are similar to the settings in [1]. At the inlet of the microchannel, the velocity is uniformly normal with a magnitude of 0.1 m/s. The inlet temperature is 25 ℃ and the bottom surface of the substrate is set as a convection boundary with a convection coefficient $h = 10$ W/(m^2 · K) and an ambient temperature of $T_{amb} = 25$ ℃. The other surfaces are treated as adiabatic. The four core processors are considered with uniform volumetric heat generation rate. Additionally, the thermal conductivity of the thermal grease is 3 W/(m · K) and the parameters of other materials are listed in Table 1.

Through thermal simulation, we aim to analyze the effects of different model parameters on the hotspot temperature of the whole structure. They include 1) the area of the core processors, 2) the pitch of core processors, 3) the total heat dissipation, and 4) the arrangements of through silicon vias (TSVs). To fulfill the aforementioned requirements, it is necessary to perform thermal simulation for 2106 cases in total.

According to the criteria discussed in Section 2.1, we categorize the device layer and die into the ROI, sort the MCHS, heat spreader and thermal interface material (TIM) layer into the top ROF, and classify the underfill with microbumps and substrate into the bottom ROF.

Table 2: CPU time comparison

	Pre-simulation	Simulation
FLUENT	None	441 h 40 m 30 s
Standard FVM	None	62 h 37 m 29 s
Proposed Method	11 m 21 s	9 m 50 s

For validation, two representative scenarios from a total of 2106 cases are performed by FLUENT, standard FVM (our in-house solver) and the proposed method respectively. When the total heat dissipation of the core processors is 30 W, the temperature results with core-concentrated TSVs and without TSVs are depicted in Figure 11. It is seen that the thermal TSVs are beneficial to reduce the hotspot temperature. Besides, it is evident that the results of the proposed method, standard FVM, and FLUENT are in very good agreement. Further, Figure 12 depicts the effect of model parameters on the hotspot temperature for the nominal TSV arrangement. In Figure 12(a), we observe that the hotspot temperature markedly decreases as the core processor area increases. From Figure 12(b), an obvious increase of the hotspot temperature is seen when the core processor pitch is too small. Again, the results of the proposed method are consistent with those of the standard FVM.

To evaluate the efficiency of the proposed method, we treat the TREND model establishment of ROFs as the pre-simulation procedure, and compare the CPU time for the total 2106 simulations, as provided in Table 2. It is worth noting that both standard FVM and the proposed method are implemented using our in-house code, ensuring the same matrix assembly approach, the same sparse linear solver and so on. This allows for a clear demonstration of the acceleration performance achieved by utilizing TREND model itself. The results present a remarkable enhancement in simulation efficiency achieved by the proposed method. When the TREND model of the ROFs is pre-built, the proposed method can achieve a speed-up of 2695x compared to FLUENT and 382x faster than standard FVM, potentially reducing thermal design timeline from weeks (441 h 40 m 30 s) to minutes (9 m 50 s). If the pre-simulation time is taken into account, it still achieves a speed-up of 1251x compared to FLUENT and 177x faster than standard FVM.

4 CONCLUSIONS

In this paper, we propose the TREND model to perform efficient and accurate thermal simulation and design of 3-D ICs and packages. The merits of the TREND models, such as the reusability and the protection of the internal details of chips and packages, demonstrate great potentials for flexible modular thermal design. The numerical results show that the proposed method achieves a speed-up of 2695x compared to FLUENT without the loss of accuracy for the thermal design of 3-D ICs with MCHS.

ACKNOWLEDGMENTS

This work was supported by National Natural Science Foundation of China (62131014, 62188102) and Program of Shanghai Academic/Technology Research Leader (23XD1401800).

REFERENCES

[1] Hitoshi Mizunuma, Yi-Chang Lu, and Chia-Lin Yang. Thermal Modeling and Analysis for 3-D ICs With Integrated Microchannel Cooling. *IEEE Transactions on Computer-Aided Design of Integrated Circuits and Systems*, 30(9):1293–1306, 2011.

[2] Yoon Jo Kim, Yogendra K. Joshi, Andrei G. Fedorov, Young-Joon Lee, and Sung-Kyu Lim. Thermal Characterization of Interlayer Microfluidic Cooling of Three-Dimensional Integrated Circuits With Nonuniform Heat Flux. *Journal of Heat Transfer*, 132(4):041009, February 2010.

[3] Swapnil S. Salvi and Ankur Jain. A Review of Recent Research on Heat Transfer in Three-Dimensional Integrated Circuits (3-D ICs). *IEEE Transactions on Components, Packaging and Manufacturing Technology*, 11(5):802–821, May 2021.

[4] Fatemeh Tavakkoli, Siavash Ebrahimi, Shujuan Wang, and Kambiz Vafai. Analysis of critical thermal issues in 3D integrated circuits. *International Journal of Heat and Mass Transfer*, 97:337–352, June 2016.

[5] Chao Wang, Xiao-Jie Huang, and Kambiz Vafai. Analysis of hotspots and cooling strategy for multilayer three-dimensional integrated circuits. *Applied Thermal Engineering*, 186:116336, March 2021.

[6] Ting Cheng, Xiaobing Luo, Suyi Huang, and Sheng Liu. Thermal analysis and optimization of multiple LED packaging based on a general analytical solution. *International Journal of Thermal Sciences*, 49(1):196–201, 2010.

[7] R. J. Moffat and A. M. Anderson. Applying Heat Transfer Coefficient Data to Electronics Cooling. *Journal of Heat Transfer*, 112(4):882–890, November 1990.

[8] Ann M. Anderson and Robert J. Moffat. The Adiabatic Heat Transfer Coefficient and the Superposition Kernel Function: Part 1—Data for Arrays of Flatpacks for Different Flow Conditions. *Journal of Electronic Packaging*, 114(1):14–21, March 1992.

[9] A. M. Anderson and R. J. Moffat. The Adiabatic Heat Transfer Coefficient and the Superposition Kernel Function: Part 2—Modeling Flatpack Data as a Function of Channel Turbulence. *Journal of Electronic Packaging*, 114(1):22–28, March 1992.

[10] Ann M. Anderson. Decoupling Convective and Conductive Heat Transfer Using the Adiabatic Heat Transfer Coefficient. *Journal of Electronic Packaging*, 116(4):310–316, December 1994.

[11] W. Nakayama and S.-H. Park. Conjugate Heat Transfer From a Single Surface-Mounted Block to Forced Convective Air Flow in a Channel. *Journal of Heat Transfer*, 118(2):301–309, May 1996.

[12] Thiago Antonini Alves and Carlos A. C. Altemani. An invariant descriptor for heaters temperature prediction in conjugate cooling. *International Journal of Thermal Sciences*, 58:92–101, 2012.

[13] Thiago Antonini Alves, Paulo H. D. Santos, and Murilo A. Barbur. An invariant descriptor for conjugate forced convection-conduction cooling of 3D protruding heaters in channel flow. *Frontiers of Mechanical Engineering*, 10(3):263–276, September 2015.

[14] Clemens J. M. Lasance. Ten Years of Boundary-Condition- Independent Compact Thermal Modeling of Electronic Parts: A Review. *Heat Transfer Engineering*, 29(2):149–168, February 2008.

[15] L. Codecasa, D. D'Amore, and P. Maffezzoni. Compact modeling of electrical devices for electrothermal analysis. *IEEE Transactions on Circuits and Systems I: Fundamental Theory and Applications*, 50(4):465–476, 2003.

[16] L. Codecasa. A novel approach for generating boundary condition independent compact dynamic thermal networks of packages. *IEEE Transactions on Components and Packaging Technologies*, 28(4):593–604, December 2005.

[17] Lorenzo Codecasa, Vincenzo d'Alessandro, Alessandro Magnani, and Niccolò Rinaldi. Compact Dynamic Modeling for Fast Simulation of Nonlinear Heat Conduction in Ultra-Thin Chip Stacking Technology. *IEEE Transactions on Components, Packaging and Manufacturing Technology*, 4(11):1785–1795, 2014.

[18] C.J.M. Lasance. Two benchmarks to facilitate the study of compact thermal modeling phenomena. *IEEE Transactions on Components and Packaging Technologies*, 24(4):559–565, 2001.

[19] Eric Monier-Vinard, Valentin Bissuel, Brice Rogié, Najib Laraqi, and Olivier Daniel. Investigation on Steady-State and Transient Boundary Condition Scenarios for Optimizing the Creation of Multiport Surrogate Thermal Models. *IEEE Transactions on Components, Packaging and Manufacturing Technology*, 8(6):1042–1055, 2018.

[20] Valentin Bissuel, Eric Monier-Vinard, Quentin Dupuis, Olivier Daniel, Najib Laraqi, and Jean-Gabriel Bauzin. Application of Stochastic Deconvolution Methods to improve the Identification of Complex BCI Multi-port Thermal RC Networks. In *2020 19th IEEE Intersociety Conference on Thermal and Thermomechanical Phenomena in Electronic Systems (ITherm)*, pages 236–243, 2020.

[21] Olaf Schenk, Klaus Gärtner, Wolfgang Fichtner, and Andreas Stricker. PARDISO: a high-performance serial and parallel sparse linear solver in semiconductor device simulation. *Future Generation Computer Systems*, 18(1):69–78, 2001.

[22] ANSYS FLUENT Software [online]. Available: http://www.ansys.com/products/fluids/ansys-fluent.

[23] Gongnan Xie, Fengli Zhang, Bengt Sundén, and Weihong Zhang. Constructal design and thermal analysis of microchannel heat sinks with multistage bifurcations in single-phase liquid flow. *Applied Thermal Engineering*, 62(2):791–802, 2014.